Remote Sensing Letters

ISSN: 2150-704X (Print) 2150-7058 (Online) Journal homepage: https://www.tandfonline.com/loi/trsl20

A fast and robust method of calculating RFM parameters for satellite imagery

Yingdan Wu & Yang Ming

To cite this article: Yingdan Wu & Yang Ming (2016) A fast and robust method of calculating RFM parameters for satellite imagery, Remote Sensing Letters, 7:12, 1112-1120, DOI: 10.1080/2150704X.2016.1219459

To link to this article: https://doi.org/10.1080/2150704X.2016.1219459

REMOTE SENSING LETTERS, 2016
VOL. 7, NO. 12, 1112–1120
http://dx.doi.org/10.1080/2150704X.2016.1219459

Taylor & Francis
Taylor & Francis Group

A fast and robust method of calculating RFM parameters for satellite imagery

Yingdan Wu [a,b] and Yang Ming [c]

[a]School of Science, Hubei University of Technology, Wuhan, China; [b]Hubei Collaborative Innovation Centre for High-efficient Utilization of Solar Energy, Hubei University of Technology, Wuhan, China; [c]CCCC Second Highway Consultants Co., Ltd, Wuhan, China

ABSTRACT

Since the normal matrix is often ill-conditioned when solving Rational Function Model (RFM) for the satellite remote sensing imagery, combining with matrix orthogonal decomposition, Levenberg–Marquardt algorithm and Compute Unified Device Architecture high-performance computing technique, a fast and robust method directly based on the error equation coefficient matrix is proposed. The method is analysed by different parameters of control point grid and compared with the common methods, namely L-curve based ridge estimation and Iteration by Correcting Characteristic Value. The experimental results show that RFM parameters derived by our method have higher fitting accuracy.

ARTICLE HISTORY
Received 13 April 2016
Accepted 26 July 2016

1. Introduction

Rational Function Model (RFM), as a kind of generic sensor model, has been widely recognized as an ideal replacement sensor model by the photogrammetry and remote sensing community and has become a state-of-art standard tool for geometric processing of high-resolution optical imagery (Hu 2001). Recently, the preliminary results demonstrated the effectiveness of using RFM as an alternative of the Range-Doppler model of Synthetic Aperture Radar (SAR) datasets (Zhang et al. 2010). Robustly and accurately solving the RFM parameters has been a hot research topic for a few decades (Fraser and Hanley 2003; Geodeckij 2003).

Nevertheless, solving the RFM parameters is essentially an ill-conditioned problem (Tao and Hu 2001a; Qin et al. 2005). Aiming that, numerous methods have been developed, which can be categorized into two broad types. The first type is to study how to reduce the number of RFM parameters in the solution process. Zhao, Liu, and Li et al. (2007) directly left out the third-order terms of the polynomials in RFM, Zhang et al. (2012) proposed a method based on scatter matrix and elimination transformation strategies, Yavari et al. (2013) advanced particle swarm optimization method, Long, Jiao, and He (2014) put forward nested regression-based optimal selection (NRBOS) and Jannati and Valadan Zoej (2015) adopted genetic modification algorithm. All

CONTACT Yingdan Wu yd_wu2010@163.com Hubei University of Technology, Wuhan, China

these studies were conducted to remove unnecessary parameters in RFM, hoping to improve the stability and the accuracy of the solution.

The second type is to investigate the way of optimum determination of RFM parameters without reduction. Most methods of this type employ the regularization techniques (Tiknonov and Arsenin 1977). Ridge estimation method is regarded as the most popular one in practical applications (Hoerl and Kennard 1970). The optimal ridge parameter determination is the key for its successful application, and a few methods have been proposed, such as ridge trace, generalized cross-validation and L-curve method (Golub 1979; Hansen 1992). Yuan and Lin (2008) applied L-curve method to determine the suitable ridge parameter in RFM parameters estimation for optical satellite remote sensing imagery, and satisfactory results are obtained. However, ridge estimation method is intrinsically biased. Aiming at this problem, Wang et al. (2001) proposed an unbiased method, namely Iteration by Correcting Characteristic Value (ICCV). The effectiveness of ICCV method in RFM parameter estimation for SAR imagery has been demonstrated by Zhang and Zhu (2008). Furthermore, Zhang et al. (2011) and Liu et al. (2012) put forward RFM calculation methods by combining the L-curve based ridge estimation method and ICCV method.

The Levenberg–Marquardt (LM) algorithm is the most popular method for solving non-linear least squares problem (Levenberg 1944; Marquardt 1963). It has been widely applied to the computer vision, close range photogrammetry, camera calibration and photo stitching (Agarwal et al. 2011). And Zhou, Jiao, and Long (2012) utilized the LM algorithm to solve the RFM parameters for SPOT-5 satellite imagery.

However, it should be noted that up to now all these studies are based on solving the normal matrix. As the condition of error equation coefficient matrix is better than that of normal matrix in general, this will ensure the solution more reliability. Therefore, a fast and robust method based directly on the error equation coefficient matrix is proposed.

2. RFM and LM algorithm

2.1. *RFM*

The RFM can be mathematically formulated as following equations (Tao and Hu 2001b):

$$\begin{cases} r = \frac{N_L(P,L,H)}{D_L(P,L,H)} \\ c = \frac{N_s(P,L,H)}{D_s(P,L,H)} \end{cases} \tag{1}$$

where (r, c) are normalized image coordinates, i.e., row and column indices of image pixels that have been offset and scaled to vary between −1.0 and +1.0. (P, L, H) represent the normalized geographic coordinates, namely latitude, longitude and elevation. N_L, D_L, N_S and D_S represent the polynomial functions of geographic coordinates taken as numerators and denominators for the ratio calculation. Frequently, three-order polynomials are adopted in the RFM, and for the two denominator polynomials, the constant term always equals 1 in order to ensure the model's consistency.

2.2. *LM algorithm*

LM algorithm is essentially on the basis of least square method introducing the step constraints. Supposing that $\Delta \boldsymbol{x}$ is iterative step for the parameters and $\Delta \boldsymbol{x}_k$ is the k-th iterative step, $\Delta \boldsymbol{x}_k$is the optimal solution of the following unconstrained convex quadratic programming problem:

$$\min \|\mathbf{B_k}\Delta \boldsymbol{x} - l_k\|^2 + u_k\|\Delta \boldsymbol{x}\|^2 \tag{2}$$

where $\mathbf{B}_k$, u_k and l_k is the error equation coefficient matrix, the damping coefficient and the constant vector in the k-th iteration, respectively. $\Delta \boldsymbol{x}_k$ can be calculated by the following formula:

$$\Delta \boldsymbol{x}_k = (\mathbf{B}^{\mathrm{T}}{}_k\mathbf{B}_k + u_k\mathbf{I})^{-1}\mathbf{B}^{\mathrm{T}}{}_k\boldsymbol{l}_k \tag{3}$$

where $\mathbf{I}$ is the unit matrix, T notation denotes the transpose of a matrix or vector. The solution vector in the k-th iteration can be derived as $\boldsymbol{x}_k = \boldsymbol{x}_{k-1} + \Delta \boldsymbol{x}_k$, where $\boldsymbol{x}_{k-1}$ is the solution vector derived from last iteration, and in an iterative way the optimal solution can be eventually obtained.

3. Our method

3.1. *Orthogonal transformation of error equation coefficient matrix*

The procedure of deriving $\Delta \boldsymbol{x}_k$ per iteration is same, and for the sake of brevity, the subscript k indicating the current iteration time is omitted in this chapter. Equation (2) can be regarded as the least square solution of the following problem:

$$\begin{bmatrix} \mathbf{B} \\ u^{1/2}I \end{bmatrix} \Delta \boldsymbol{x} \cong \begin{bmatrix} \boldsymbol{l} \\ 0 \end{bmatrix} \tag{4}$$

Firstly, the QR factorization with column pivoting (QRP) of $\mathbf{B}$ is performed by the Householder transformation, that is $\mathbf{Q}^{\mathrm{T}}\mathbf{B}\mathbf{P} = \begin{bmatrix} \mathbf{R} \\ 0 \end{bmatrix}$, where $\mathbf{Q}$ is orthogonal matrix, which is the product of a series of Householder transformation matrices, $\mathbf{P}$ is the permutation matrix and $\mathbf{R}$ is the non-singular upper triangular matrix of rank($\mathbf{A}$) order, that is rank($\mathbf{R}$) = rank($\mathbf{A}$). Apply the matrix $\mathbf{Q}$ and $\mathbf{P}$ to the error equation coefficient matrix $\mathbf{B}$ and the constant vector $\boldsymbol{l}$:

$$\begin{bmatrix} \mathbf{Q}^{\mathrm{T}} & 0 \\ 0 & \mathbf{P}^{\mathrm{T}} \end{bmatrix} \begin{bmatrix} \mathbf{B} \\ u^{1/2}\mathbf{I} \end{bmatrix} \mathbf{P} = \begin{bmatrix} \mathbf{R} \\ 0 \\ u^{1/2}\mathbf{I} \end{bmatrix}, \begin{bmatrix} \mathbf{Q}^{\mathrm{T}} & 0 \\ 0 & \mathbf{P}^{\mathrm{T}} \end{bmatrix} \begin{bmatrix} l \\ 0 \end{bmatrix} = \begin{bmatrix} \mathbf{Q}^{\mathrm{T}}\boldsymbol{l} \\ 0 \end{bmatrix} \tag{5}$$

then we can get:

$$\begin{bmatrix} \mathbf{R} \\ 0 \\ u^{1/2}\mathbf{I} \end{bmatrix} \mathbf{P}^{\mathrm{T}}\Delta \boldsymbol{x} = \begin{bmatrix} \mathbf{Q}^{\mathrm{T}}l \\ 0 \end{bmatrix} \tag{6}$$

When the condition of error equation coefficient matrix **B** is well, damping coefficient u is set to be zero, the solution of Equation (6) is $\Delta \boldsymbol{x} = \mathbf{P}\mathbf{R}^{-1}(\mathbf{Q}^{\mathrm{T}}l)_{(1:n)}$, where $(\mathbf{Q}^{\mathrm{T}}l)_{(1:n)}$ represents the vector formed by the first n elements of $\mathbf{Q}^{\mathrm{T}}l$.

When **B** is ill-conditioned, u is larger than zero. In this situation, the coefficient matrix and constant vector in Equation (6) will be further processed by Givens transformation. Given that the product of a series of Givens transformation matrices is **G**, we can get:

$$\mathbf{G}\begin{bmatrix}\mathbf{R}\\0\\u^{1/2}\mathbf{I}\end{bmatrix} = \begin{bmatrix}\mathbf{R}'\\0\end{bmatrix}, \mathbf{G}\begin{bmatrix}\mathbf{Q}^{T}l\\0\end{bmatrix} = \begin{bmatrix}\boldsymbol{\alpha}\\\boldsymbol{\beta}\end{bmatrix} \tag{7}$$

where $\mathbf{R}'$ is the non-singular triangular matrix. The solution of Equation (6) is $\Delta \boldsymbol{x} = \mathbf{P}\mathbf{R}'^{-1}\alpha$.

3.2. *Adjustment of damping coefficient*

Determining suitable damping coefficient is of cardinal significance for LM algorithm. The adaptive strategy as follows is adopted in this article (Keyvan and Faramarz 2015):

$$u_k = \lambda_k \|\boldsymbol{I}_k\|^{\delta_k}, \delta^k = \begin{cases} \frac{1}{\|\boldsymbol{I}_k\|} \text{if} \|\boldsymbol{I}_k\| \geq 1 \\ 1 + \frac{1}{k} \text{otherwise} \end{cases} \tag{8}$$

where k is the current iteration time and λ_k is the adaptive factor. It is noticeable that even if $\|I_k\|$ is very large, $u_k = \lambda_k \|I_k\|^{1/\|I_k\|}$ is not large and so the LM step is not small too. This causes the algorithm moving fast to the solution set.

To determine the value of adaptive factor λ_k, ρ_k is firstly calculated, which is defined as follows:

$$\rho_k = \frac{\|I_k\|_2^2 - \|\mathrm{F}(\boldsymbol{x}_k + \Delta \boldsymbol{x}_k)\|_2^2}{\|I_k\|_2^2 - \|\mathbf{B}_k \Delta \boldsymbol{x}_k - \boldsymbol{I}_k\|_2^2} \tag{9}$$

ρ_k can be considered as the indicator that how well the current linear model approximates the target function $\mathrm{F}(\cdot)$ as described in Equation (1). A large value of ρ_k indicates good approximation, and λ_k should decrease so that next LM step is closer to the Gauss–Newton step. The updating strategy of λ_k is as follows:

$$\lambda_k = \begin{cases} 0.1\lambda_k & \rho_k > 0.75 \\ \lambda_k & 0.25 \leq \rho_k \leq 0.75 \\ 10\lambda_k & \rho_k < 0.25 \end{cases} \tag{10}$$

3.3. *Acceleration by CUDA*

QRP is an efficient way for computing a rank revealing QR factorization in this article. However, it is computationally expensive. Graphic processing units (GPUs) have high memory bandwidth and more floating point units as compared to the central processing unit. Compute Unified Device Architecture (CUDA) programming model organizes a parallel computation using the abstractions of threads, blocks and grids, and it allows

us to execute thousands of threads simultaneously on the GPU. To improve calculation efficiency of our method, parallel algorithm for QRP proposed by the Tomas, Bai, and Hernandez (2012) is adopted.

4. Experiments and analysis

4.1. *Description of datasets and test design*

In order to verify the method proposed in this article, ENVISAT SAR imagery as well as high-resolution optical imagery WorldView-1 are tested. The size of ENVISAT imagery is 5170 × 26895 pixels, and the area covered by it is some place in Sichuan province in China, which is hilly with height ranging from 341 to 967 m. For WorldView-1 imagery, its image size is 34771 × 14272 pixels, covering a typically mountainous area of Qinghai province with height varying between 2870 and 3368 m.

In the test, control point grid and check point grid are firstly built up. For them, the grid number and the number of elevation layer are two important parameters. Grid number of $m \times m$ means that the object space covered by the image is divided into $m \times m$ cells, and the virtual ground points are distributed regularly within the 3D object space. Grid number and number of elevation layer for the check point grid are double of that of the control point grid, and the offset of x and y coordinates between check point grid and control point grid is half of width and height of the check cell, respectively. Image coordinates derived by the solved RFM parameters are compared with those by the physical sensor model, and the root mean square error (RMSE) is chosen as the measurement to evaluate the fitting accuracy.

4.2. *Test for different control point grid parameters*

Firstly, the number of elevation layer is fixed as 5, the grid number is set to be 10 × 10、20 × 20、30 × 30、40 × 40、50 × 50、60 × 60、70 × 70、80 × 80, respectively. The fitting accuracy of our method is illustrated in Figure 1. As results shown, the fitting RMSEs are decreasing as increasing the grid number, and become stable after 40 × 40.

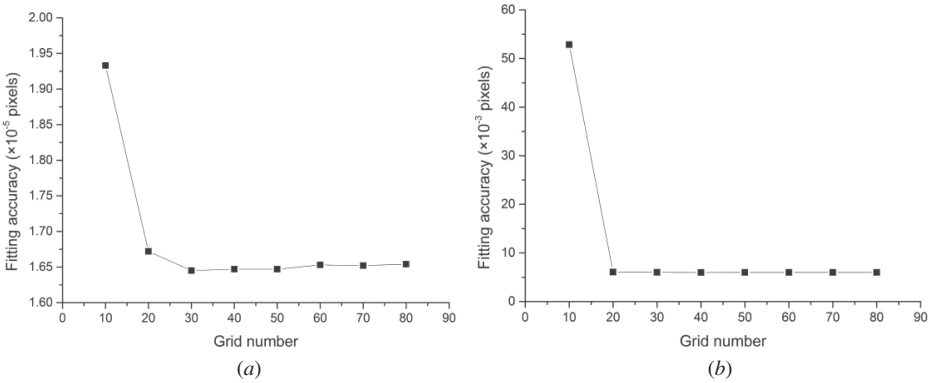

Figure 1. Planemetric accuracy of different grid numbers for the Envisat SAR and WorldView-1 data: (a) Envisat SAR; (b) WorldView-1.

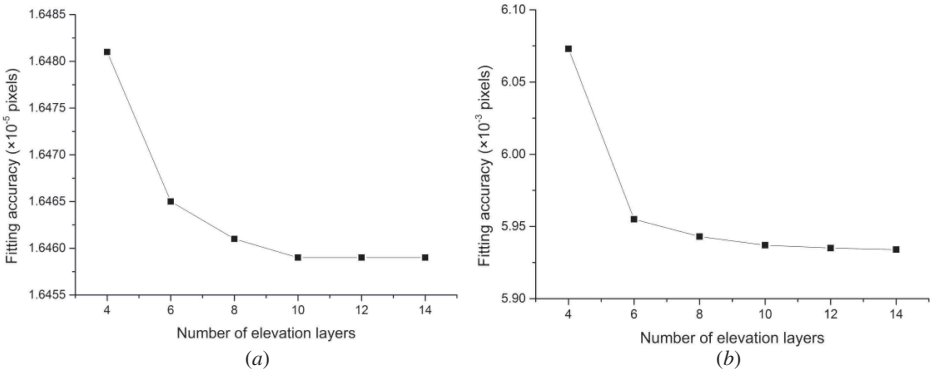

Figure 2. Planemetric accuracy of different number of elevation layers for the Envisat SAR and WorldView-1 data: (a) Envisat SAR; (b) WorldView-1.

Then, the grid number is fixed as 40 × 40, the number of elevation layer is set to be 4, 6, 8, 10, 12 and 14 respectively, and the result is shown in Figure 2. The fitting RMSEs are gradually reduced along with increasing the number of elevation layer, and reach steady after 10. Therefore, the grid number and the number of elevation layer for the control point grid can be set as 40 × 40 and 10, respectively, for the sake of keeping high fitting accuracy and saving computation time cost.

4.3. *Comparison with common methods*

Using the parameters of control point grid determined earlier, virtual control points and virtual check points are generated. The same control points and check points are used to compare our method with other conventional methods, such as L-curve based ridge estimation method (Hansen 1992) and ICCV method (Wang et al. 2001). For the L-curve-based ridge estimation method (L-curve, for short), ridge parameter derived is 0.0000148. For the ICCV method, the threshold for the maximum absolute value of parameter changing and iteration number is set to be 1×10^{-9} and 50,000, respectively. For our method, initial value of adaptive factor $\lambda^{(0)}$ is set to be 0.01, the threshold for the maximum absolute value of parameter changing and iteration number is set to be 1×10^{-10} and 200, respectively. The comparison results of different methods are illustrated in the Table 1, in which the cost time with superscript * denotes that it is calculated if CUDA technique is not used for our method.

Table 1. Comparison of different methods for the Envisat SAR dataset and WorldView-1 imagery.

		Method		
Results		L-curve	ICCV	Our method
ENVISAT	Time (s)	1.93	244.22	2.14/4.24*
	Sample ($\times 10^{-5}$ pixels)	5.362	5.292	1.646
	Line ($\times 10^{-5}$ pixels)	45.01	0.163	0.009
	Plane ($\times 10^{-5}$ pixels)	45.33	5.295	1.646
WorldView-1	Time (s)	1.15	217.03	1.35/2.25*
	Sample ($\times 10^{-3}$ pixels)	6.948	6.988	5.101
	Line ($\times 10^{-3}$ pixels)	3.205	3.200	3.037
	Plane ($\times 10^{-3}$ pixels)	7.652	7.686	5.937

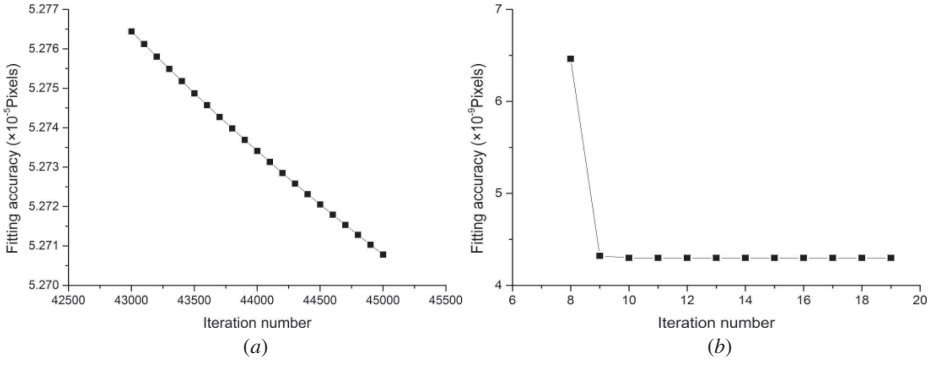

Figure 3. Convergence of the last iterations: (a) ICCV; (b) our method.

Taking Envisat SAR imagery for example, L-curve method needs no iteration, ICCV method converges after 45,051 iterations and our method only after 19 iterations. The convergence situation of the last iterations for ICCV method and our method is shown in Figure 3.

Through the results of Table 1 and Figure 3, following conclusions can be drawn:

(1) The fitting accuracy of the RFM parameters derived by our method is very high, that is, 1.646×10^{-5} pixels and 5.937×10^{-3} pixels for Envisat SAR dataset and WorldView-1 imagery, respectively. The conventional methods, namely L-curve and ICCV method, also have obtained good fitting accuracy, both better than the practical requirement of 0.01 pixels.

(2) Compared with the L-curve and ICCV method, our method has gained better fitting accuracy. For Envisat SAR imagery, the conditional number of the original normal matrix reaches 9.0×10^{15}. L-curve method decreases it to 5.3×10^{9} by adding the ridge parameter to each diagonal elements of the normal matrix. In the same way, ICCV method decreases the conditional number of normal matrix to 2.2×10^{4} by adding a constant 1. For our method, due to the fact that it is based on the error equation coefficient matrix, the conditional number of solving equation is ranging from 3.4×10^{8} to 1.5×10^{6}. For the L-curve method, the optimum ridge parameter is determined by sampling of different ridge parameters, 10 samples performed in this article, but this cannot take into account the actual condition of normal matrix in the process of iteration. In addition, the ridge parameter substantially biases the normal matrix. Therefore, the results of L-curve method are worse than those of other methods. Though the ICCV method is theoretically unbiased, its spectral radius is near to 1, resulting in low convergent rate, over 40,000 iteration times needed in the letter. Moreover, the results of the ordinary least square method are taken as the initial value for the ICCV method, which is far away from the correct solution set, resulting in the optimal solution difficult to reach. For our method, through matrix decomposing technique and adaptive adjustment of the damping parameter, the ill-posed problem is thoroughly considered in the entire process. And damping parameter can be flexibly adjusted depending on the condition of error equation coefficient matrix in the process of iteration. All these strategies enable the algorithm to have a fast convergent rate between the steepest descent method and Gauss–Newton method and have enhanced reliability in the numerical calculation.

(3) Using the same original data and computing environment, L-curve method takes the least time as no iteration is needed, and ICCV method costs most. With acceleration

of CUDA on the QRP, significant improvement has been gained, and the speed of our method is at the same level as that of L-curve method.

5. Conclusions

In this article, a fast and robust RFM parameter estimation method directly based on the error equation is proposed, which combines the orthogonal decomposition methods, Levenberg–Marquardt algorithm and CUDA technique. Through the experiment on SAR dataset and optical satellite imagery, the suitable parameters of control point grid for the proposed method are studied, and by comparing with common methods, such as L-curve based ridge estimation and ICCV, it is shown that our method can get better fitting accuracy, and the speed is also very fast.

Disclosure statement

No potential conflict of interest was reported by the authors.

Funding

The research was supported by the National Natural Science Foundation of China [61301278]; Scientific Research Starting Foundation for Doctors, Hubei University of Technology [BSQD12078]; Open Foundation of Hubei Collaborative Innovation Centre for High-efficient Utilization of Solar Energy [HBSKFM2014001].

ORCID

Yingdan Wu http://orcid.org/0000-0002-2815-6694
Yang Ming http://orcid.org/0000-0002-1131-6858

References

Agarwal, S., Y. Furukawa, N. Snavely, I. Simon, B. Curless, S. M. Seitz, and R. Szeliski. 2011. "Building Rome in a Day." *Communications of the ACM* 54 (10): 105–112. doi:10.1145/2001269.

Fraser, C. S., and H. B. Hanley. 2003. "Bias Compensation in Rational Functions for IKONOS Satellite Imagery." *Photogrammetric Engineering & Remote Sensing* 69 (1): 53–57. doi:10.14358/PERS.69.1.53.

Geodeckij, D. 2003. "Block Adjustment of High Resolution Satellite Images Described by Rational Functions." *Photogrammetric Engineering and Remote Sensing* 69 (1): 59–68. doi:10.14358/PERS.69.1.59.

Golub, G. H. 1979. "Generalized Corss-validation as a Method for Choosing a Good Ridge Parameter." *Technometrics* 21 (2): 215–223. doi:10.1080/00401706.1979.10489751.

Hansen, P. C. 1992. "Analysis of Discrete Ill-posed Problems by Means of the L-curve." *SIAM Review* 34 (4): 561–580. doi:10.1137/1034115.

Hoerl, A. E., and R. W. Kennard. 1970. "Ridge Regression Biased Estimation for Non-Orthogonal Problems." *Technimetrics* 8 (1): 27–51.

Hu, Y. 2001. "A Comprehensive Study on the Rational Function Model for Photogrammetric Processing." *Photogrammetric Engineering and Remote Sensing* 67 (12): 1347–1357.

Jannati, M., and M. J. Valadan Zoej. 2015. "Introducing Genetic Modification Concept to Optimize Rational Function Models (RFMs) for Georeferencing of Satellite Imagery." *GIScience & Remote Sensing* 52 (4): 510–525. doi:10.1080/15481603.2015.1052634.

Keyvan, A., and R. Faramarz. 2015. "A Modified Two Steps Levenberg-Marquardt Method for Nonlinear Equations." *Journal of Computational and Applied Mathematics* 288 (2015): 341–350. doi:10.1016/j.cam.2015.04.040.

Levenberg, K. 1944. "A Method for the Solution of Certain Non-Linear Problems in Least Squares." *Quarterly of Applied Mathematics* 2: 164–168.

Liu, B., J. Gong, W. Jiang, and X. Y. Zhu. 2012. "Improvement of the Iteration by Correcting Characteristic Value Based on Ridge Estimation and Its Application in RPC Calculating." *Geomatics and Information Science of Wuhan University* 37 (4): 399–403.

Long, T., W. Jiao, and G. He. 2014. "Nested Regression Based Optimal Selection (NRBOS) of Rational Polynomial Coefficients." *Photogrammetric Engineering & Remote Sensing* 80 (3): 261–269. doi:10.14358/PERS.80.3.261.

Marquardt, D. 1963. "An Algorithm for Least Squares Estimation on Nonlinear Parmeters." *SIAM Journal on Applied Mathematics* 11 (1): 431–441. doi:10.1137/0111030.

Qin, X. W., S. F. Tian, Y. T. Hong, and G. Zhang. 2005. "The Algorithm for Parameters of RPC Model Without Initial Value." *Remote Sensing for Land & Resources* 2005 (4): 7–10.

Tao, C. V., and Y. Hu. 2001a. "A Comprehensive Study on the Rational Function Model for Photogrammetric Processing." *Photogrammetric Engineering and Remote Sensing* 67 (12): 1347–1357.

Tao, C. V., and Y. Hu. 2001b. "Use of the Rational Function Model for Image Rectification." *Canadian Journal of Remote Sensing* 27 (6): 593–602. doi:10.1080/07038992.2001.10854900.

Tikhonov, A. N., and V. Y. Arsenin. 1977. *Solutions of Ill-Posed Problems*. Washington: Winston & Sons.

Tomas, A., Z. J. Bai, and V. Hernandez. 2012. "Parallelization of the QR Decomposition with Column Pivoting Using Column Cyclis Distribution on Multicore and GPU Processors." *Lecture Notes in Computer Science* 7851: 50–58.

Wang, X. Z., D. Y. Liu, Q. Y. Zhang, and H. L. Huang. 2001. "The Iteration by Correcting Characteristic Value and Its Application in Surveying Data Processing." *Journal of Heilongjiang Institute of Technology* 15 (2): 3–6.

Yavari, S., M. J. Valadan Zoej, A. Mohammadzadeh, and M. Mokhtarzade. 2013. "Particle Swarm Optimization of RFM for Georeferencing of Satellite Images." *IEEE Geoscience and Remote Sensing Letters* 10 (1): 135–139. doi:10.1109/LGRS.2012.2195153.

Yuan, X. X., and X. Y. Lin. 2008. "A Method for Solving Rational Polynomial Coefficients Based on Ridge Estimation." *Geomatics and Information Science of Wuhan University* 33 (11): 1130–1133.

Zhang, G., W. B. Fei, Z. Li, X. Y. Zhu, and X. M. Tang. 2010. "Analysis and Test of the Substitutability of the RPC Model for the Rigorous Sensor Model of Spaceborne SAR Imagery." *Acta Geodaetica et Cartographica Sinica* 39 (3): 264–270.

Zhang, G., and X. Y. Zhu. 2008. "A Study of the RPC Model of TerraSAR-X and COSMO-SKYMED SAR Imagery." In *Proc. Int. Arch. Photogramm., Remote Sens. Spatial Inf. Sci.*, 321–324. ISPRS.

Zhang, L., X. Y. He, T. Balz, X. H. Wei, and M. S. Liao. 2011. "Rational Function Modeling for Spaceborne SAR Datasets." *ISPRS Journal of Photogrammetry and Remote Sensing* 66 (1): 133–145. doi:10.1016/j.isprsjprs.2010.10.007.

Zhao, L. P., F. D. Liu, L. Jian, and W. Wang. 2007. "Research on Reducing Term of High Order in RFM Model." *Science of Surveying and Mapping* 32 (4): 14–17.

Zhang, Y. J., Y. H. Lu, L. Wang, and X. Huang. 2012. "A New Approach on Optimization of the Rational Function Model of High-Resolution Satellite Imagery." *IEEE Transactions on Geoscience and Remote Sensing* 50 (7): 2758–2764. doi:10.1109/TGRS.2011.2174797.

Zhou, Q., W. L. Jiao, and T. F. Long. 2012. "Solution to the Rational Function Model Based on the Levenberg-Marquardt Algorithm." *The 9th International Conference on Fuzzy Systems and Knowledge Discovery*, Chongqing, China, May 29–31, 2795–2799.